Journal of Power Sources 195 (2010) 3077–3083

Contents lists available at ScienceDirect

Journal of Power Sources

journal homepage: www.elsevier.com/locate/jpowsour

Proton exchange membranes based on semi-interpenetrating polymer networks of fluorine-containing polyimide and Nafion®

Haiyan Pan, Hongting Pu*, Decheng Wan, Ming Jin, Zhihong Chang

Institute of Functional Polymers, School of Materials Science & Engineering, Tongji University, Shanghai 200092, PR China

ARTICLE INFO

Article history:
Received 13 October 2009
Received in revised form
16 November 2009
Accepted 25 November 2009
Available online 1 December 2009

Keywords:
Fluorine-containing polyimide
Nafion®
Proton exchange membrane
Semi-IPN
Proton conductivity

ABSTRACT

A series of reinforced composite membranes as proton exchange membranes were prepared from Nafion®212 and crosslinkable fluorine-containing polyimides (FPI). FPI was prepared from the polymerization of 4,4′-(hexafluoroisopropylidene) diphthalic anhydride (6FDA), 2,2′-bis(trifluoromethyl)-4,4′-diaminobiphenyl (TFMB), and 3,5-diaminobenzoic acid (DABA). Then FPI was thermally crosslinked during the membrane preparation and formed the semi-interpenetrating polymer networks (semi-IPN) structure in the composite membranes. The thermal properties of the composite membranes were characterized by thermogravimetric analysis. The crosslinking density of FPI in the composite membranes was evaluated by the gel fraction. These membranes showed excellent thermal stabilities and good oxidative stabilities. Compared with Nafion®212, the obtained composite membranes displayed much improved mechanical properties and dimensional stabilities. The tensile strength of the composite membranes was more than twice that of Nafion®212. The composite membranes exhibited high proton conductivity, which ranged from 2.3×10^{-2} S cm^{-1} to 9.1×10^{-2} S cm^{-1}. All membranes showed an increase in proton conductivity with temperature elevation.

1. Introduction

As one of the key component of polymer electrolyte membrane fuel cells (PEMFCs), proton exchange membranes (PEMs) have to combine various properties such as excellent chemical stability especially against oxygen and free radicals, mechanical stability with reasonable swelling ratio as well as high proton conductivity [1–5]. Perfluorinated sulfonic acid polymers, such as Nafion® membranes, were the most commonly used materials in practical systems for their high proton conductivity and extremely high oxidative stability. However, due to the poor dimensional stability, low mechanical properties of Nafion® at high humidity and high temperature, as well as high cost, an essential need for cost-effective and reinforced substitutes with improved performance arises [6–9]. Nafion® blended with the second component could not only reduce the cost, but also improve the mechanical properties and the dimensional stability. Recently, the reinforced composite membranes based on Nafion® mainly include Nafion®/PTFE (porous) composite, Nafion®/PTFE (fibrous) composite membranes, and Nafion®/carbon nanotubes composite membranes [10–19]. The introduction of the non-conducting components will reduce the proton conductance of the composite membranes. However, the proton conductance of the composite membrane could be improved by reducing the thickness of the membrane if the mechanical property of the membrane is good enough. Nevertheless, the mechanical properties of the porous and fibrous PTFE are limited.

Aromatic polyimide is a class of high performance engineering plastics with high tensile strength, unique heat resistance, as well as excellent chemical and oxidative stabilities, etc. [20,21]. The composite membranes based on crosslinkable polyimide and Nafion® can form semi-interpenetrating polymer networks (semi-IPN) within the membranes. The composite membranes with semi-IPN structure could greatly improve the mechanical properties and the dimensional stability of pure Nafion®. In this work, the fluorine-containing polyimide with reactive carboxyl groups (FPI) was synthesized via 'one-pot' method. The bond energy of C–F is much higher than that of C–H bond, which gives the better chemical stability of C–F bond than that of C–H bond. By solution casting method, a new kind of PEMs based on FPI and Nafion®212 was prepared. The carboxyl group of FPI reacted with diethylene glycol (EG) at high temperature during the membrane preparation, which formed the semi-IPN structure of the composite membranes. The mechanical properties, proton conductivity, oxidative stability of these composite membranes were also investigated systematically.

* Corresponding author. Tel.: +86 21 65982461; fax: +86 21 65982461.
E-mail address: puhongting@tongji.edu.cn (H. Pu).

0378-7753/$ – see front matter © 2009 Elsevier B.V. All rights reserved.
doi:10.1016/j.jpowsour.2009.11.116

2. Experimental

2.1. Materials

3,5-Diaminobenzoic acid (DABA) was purchased from Shanghai Bangcheng Chem. Co. 4,4′-(Hexafluoroisopropylidene) diphthalic anhydride (6FDA, >99%) and 2,2′-bis(trifluoromethyl)-4,4′-diaminobiphenyl (TFMB, >98%) were purchased from Shanghai Darui Fine Chem. Co., and both of them were used as received. Nafion®212 was from DuPont Co. N-Methylpyrrolidone (NMP), isoquinoline (spectroscopically pure), methanol (99.7 wt%, AR grade), and diethylene glycol (EG) were supplied by Shanghai Chemical Reagent Co.

2.2. Synthesis of crosslinkable polyimide

A synthetic procedure of crosslinkable fluorine-containing polyimide was described below using starting monomers of 6FDA/TFMB/DABA (10/9/1, mol/mol) as an example. To a 100 mL completely dried three-necked flask, which was equipped with a mechanical stirring device, condenser and a nitrogen inlet, 3 mmol 6FDA, 2.7 mmol TFMB, 12 mL NMP, and 0.78 mL isoquinoline were added. After the mixture was stirred under nitrogen flow at room temperature for 8 h, 0.3 mmol DABA was added and stirred at room temperature for another 8 h. Then the mixture was heated at 200 °C for 12 h. After cooled to 100 °C, the mixture was poured into 200 mL methanol. The fiber-like precipitate was filtered off, washed with methanol thoroughly, and dried in vacuum at 120 °C for 24 h. The synthetic scheme and chemical structure of the crosslinkable polyimide was shown in Fig. 1. FPI with different DABA content is named FPI-*X*, in which *X* represents the mole percentage of DABA.

2.3. Preparation and crosslinking of the composite membrane

The composite membranes are named CM-*X*–*Y*, in which *Y* represents the weight ratio of FPI-*X* in the composite membranes, and *X* is the mole percentage of DABA in FPI as mentioned before. At the same time, UCM-10–15 (uncrosslinked CM-10–15) was also prepared as a comparison. A preparation procedure of the composite membranes is described below using CM-10–15 as an example. 0.15 g FPI and 0.85 g Nafion®212 were dissolved in 9 mL NMP. Then 0.9 mL diethylene glycol (EG) was added to the solution. The mixture was stirred at room temperature until EG was dissolved in NMP completely. The solution was cast on glass plates at 80 °C for 10 h to evaporate the solvent, and then heated at 150 °C for 24 h in vacuum. Then the plates were put into the deionized water until the film fell off naturally and dried in vacuum at 150 °C for 24 h.

2.4. Characterization of the membranes

2.4.1. Fourier-transform infrared

FTIR analysis of the membranes was carried out by a thermo Bruker EQUINOXSS/HYPERION2000 spectrometer. KBr pellet method was used.

2.4.2. ^1H NMR

^{1}H NMR spectra of the polymers in deuterated dimethyl sulfoxide (DMSO) were recorded on a Varian Bruker AC-250 instrument.

2.4.3. Gel fraction

Gel fractions of the crosslinked networks were measured by solvent extraction [22,23]. 0.1–0.3 g sample was placed in dimethyl sulfoxide (DMSO) and Soxhlet extracting for 24 h. After removal of the solvent by drying at 120 °C for 24 h under vacuum, the remaining mass was weighed as gel. Gel fractions were calculated by dividing the weights of the gels by the initial weights of the networks.

2.4.4. Thermal analysis

Thermogravimetric analyzer (TGA) results of the membranes were measured with a STA 449C (Netzsch Co.) in the temperature range from 90 °C to 700 °C at a heating rate of 10 °C min^{-1} under nitrogen atmosphere.

2.4.5. Tensile properties

Tensile properties of the composite membranes were performed on a universal material testing machine (DXLL-5000) at a strain speed of 50 mm min^{-1} at room temperature according to ASTM D882-02.

2.4.6. Dynamic mechanical analysis

Dynamic mechanical analysis (DMA) was performed with a TA Instruments DMA 2980 mechanical spectrometer under nitrogen in tension mode, at a frequency of 1.0 Hz and a heating rate of 10 °C min^{-1}. The initial static force was set to be 1.0N.

2.4.7. Water uptake

The measurement of the water uptake of the membranes were carried out by immersing three sheets of membranes (20–30 mg per sheet) into water at 25 °C and 80 °C for 48 h, before which the membranes were dried under vacuum at 100 °C for 2 days and weighed. Then the membranes were taken out, wiped with tissue paper, and quickly weighed on a microbalance. The water uptake (WU) of the membranes was calculated from Eq. (1) [24,25]:

$$\mathrm{WU}\,(\%) = \frac{W_{\mathrm{wet}} - W_{\mathrm{dry}}}{W_{\mathrm{dry}}} \times 100 \quad (1)$$

where W_{dry} and W_{wet} are the data of dry and corresponding wet membrane sheets, respectively. The water uptake of the membranes was estimated from the average value of at least three measurements for each sheet.

2.4.8. Swelling ratio

Before the measurement, the membranes were dried under vacuum at 100 °C for 2 days and the length and the thickness of the membranes were measured. Similar to the water uptake, the measurement of the swelling ratio of the membranes was carried out by immersing three sheets of membranes (20–30 mg per sheet) into water at 25 °C and 80 °C for 5 h, respectively. Then the membranes were taken out. The length of the swollen membrane was measured by vernier caliper. Swelling ratio (SR) of the membranes was calculated from Eq. (2) [26]:

$$\mathrm{SR}\,(\%) = \frac{L_{\mathrm{wet}} - L_{\mathrm{dry}}}{L_{\mathrm{dry}}} \times 100 \quad (2)$$

where L_{dry} and L_{wet} are the length of dry and swollen membranes, respectively. Swelling ratio of the membranes was estimated from the average value of at least three measurements for each sheet.

2.4.9. Proton conductivity

The proton conductivity (σ) of the composite membranes was measured by Electrochemical Impedance Lab CHI 604B (CH Instruments Inc.), which worked in the galvanostatic mode and produced a proton current across the membrane. The test cell (Fig. 2) was placed in a thermo-controlled water bath for measurement at relatively humidity (RH) of 100%. The proton conductivity of the composite membranes was measured at different temperatures. σ_{DC} was determined from Eq. (3):

$$\sigma_{\mathrm{DC}} = \frac{d}{SZ} \quad (3)$$

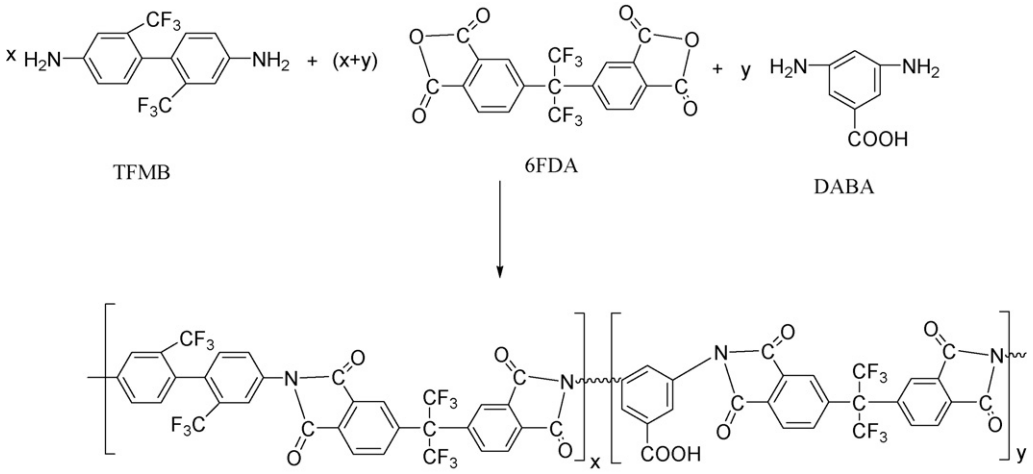

Fig. 1. Synthetic procedure of fluorine-containing polyimide with reactive carboxyl groups.

where d is the distance between the two electrodes and S is the sectional area of the membrane, Z is the measured impedance of the membrane.

2.4.10. Oxidative stability

The oxidative stability of the composite membranes was examined by immersing the membranes in Fenton reagent (30 ppm $FeSO_4$ in 30% H_2O_2) at room temperature [27]. Oxidative stability of the membranes was characterized by the elapsed time that the membranes started to become a little brittle (the membranes were broken after being drastically shaken).

3. Results and discussion

3.1. Synthesis of fluorine-containing polyimide with reactive carboxyl groups

As depicted in Fig. 1, the fluorine-containing polyimide was synthesized by copolymerization of 6FDA, TFMB, and DABA. By changing the mole ratio of TFMB and DABA, a series of FPI with different DABA content ranging from 0% to 30% (mol%) were obtained. The monomer feed ratio of FPI-*X* was listed in Table 1. The chemical structure of FPI-*X* was characterized by FTIR and shown in Fig. 3. The absorption bands at 1785 cm^{-1} and 1726 cm^{-1} were assigned to the stretch vibration of carbonyl groups of imide ring. The C–N–C stretching vibration of the imide ring was observed around 1364 cm^{-1}. Compared to FTIR spectrum of FPI-0, the peak at 1462 cm^{-1} and 649 cm^{-1} of FPI-*X* (*X* = 10, 20, 30) was attributed to the vibration of O=C–O and O–H in the carboxyl group. To FPI-10, FPI-20, and FPI-30, the absorption band at 1462 cm^{-1} was getting stronger with increasing DABA contents. Fig. 4 shows the ^1H NMR spectrum of FPI-10. The signals at 7.5–8.2 ppm are assigned to the Ar–H bond. The peaks at 11.0 ppm were attributed to the carboxyl group. Therefore, it could safely conclude that the carboxyl group has been imported to FPI successfully.

Table 1
The monomer feed ratio in the synthesis of fluorine-containing polyimide.

Polyimide	6FDA (mol)	TFMB(mol)	DABA(mol)	*X*% (DABA/6FDA, mol/mol)
FPI-0	10	10	0	0
FPI-5	10	9.5	0.5	5
FPI-10	10	9.0	1.0	10
FPI-15	10	8.5	1.5	15
FPI-20	10	8.0	2.0	20
FPI-30	10	7.0	3.0	30

3.2. Crosslinking and gel fraction of the composite membranes

By changing the weight ratio of FPI-*X* and Nafion®212 in the membrane preparation, a series of composite membranes with different contents of FPI-*X* were obtained. The content of FPI-*X* in the composite membranes can range from 5% to 30% (wt%) for the

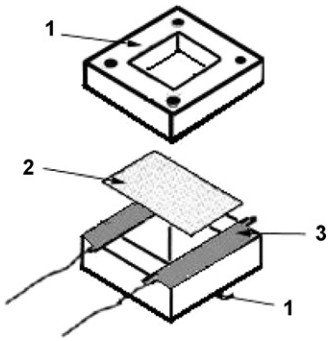

Fig. 2. Cell used for determination of membrane conductivity: (1) Teflon® block, (2) membrane sample and (3) blackened Pt foil.

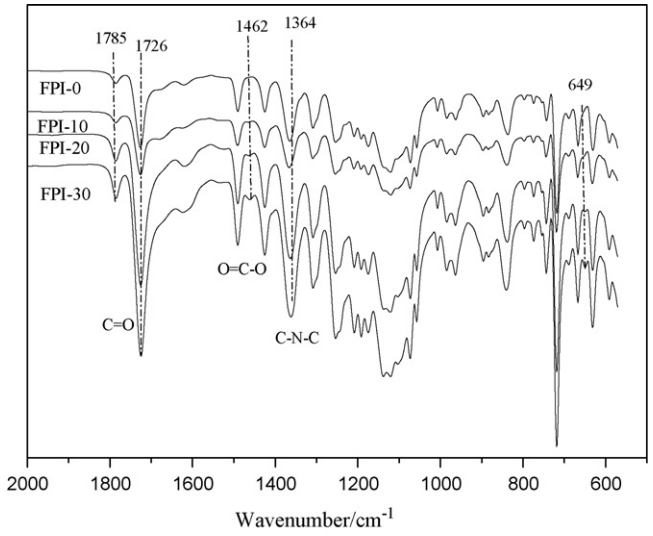

Fig. 3. FTIR spectrum of crosslinkable fluorine-containing polyimide (FPI-*X*) with reactive carboxyl groups.

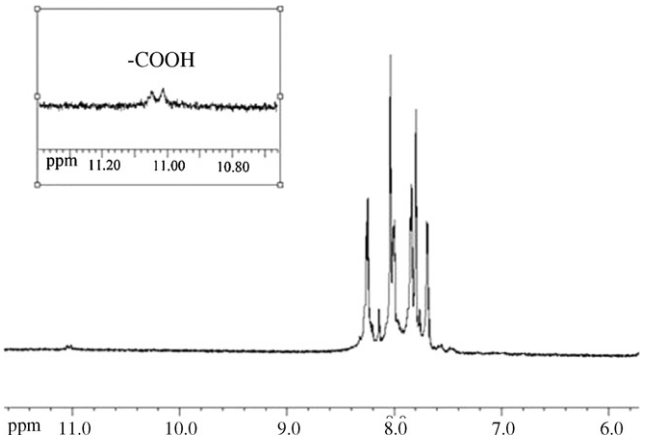

Fig. 4. ^{1}H NMR spectrum of crosslinkable fluorine-containing polyimide (FPI-10) with reactive carboxyl groups.

purpose to insure the membrane with relatively high mechanical properties and proton conductivity. During the membrane preparation, the carboxyl in FPI can react with diethylene glycol (EG) at high temperature and form the semi-IPN structure (Fig. 5) within the composite membranes.

Gel fraction of the crosslinked networks can be regarded as an indirect method for assessing the degree of crosslinking. The measured gel fraction of the crosslinked membranes are given in Table 2. As expected, the gel fraction of CM-*X*–15 increases with increasing content of the carboxyl groups in FPI-*X* when *Y* equals to 15. This proves that the carboxyl group in FPI can react with EG and form networks. The higher the content of the carboxyl group in FPI-*X*-15 is, the higher the crosslinking degree of the composite membranes is. For CM-10–*Y* series membranes, the gel fraction decreases with increasing content of FPI-10 or with decreasing content of Nafion®212. This might be attributed to the reason that the existence of the sulfonic group in Nafion®212 could catalyze the crosslinking reaction.

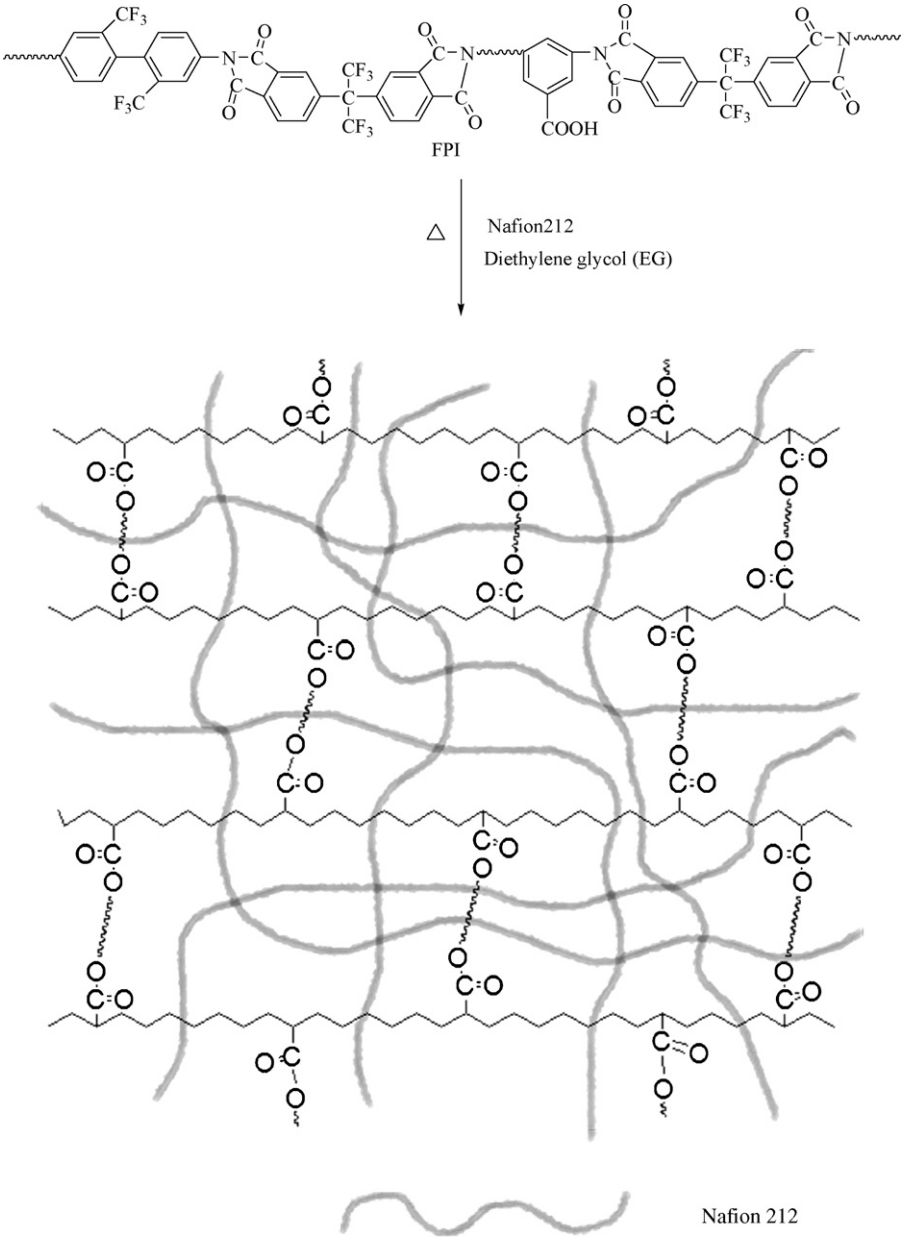

Fig. 5. Semi-IPN structure of the FPI/Nafion®212 composite membrane.

Table 2
Gel fractions of the composite membranes.

Membranes	Content of carboxyl groups in FPI (*X*, mol%)	Content of FPI-*X* in membranes (*Y*, wt%)	Nafion®212 (wt%)	Gel fraction (%)
CM-10–5	10	5	95	94.6
CM-10–10	10	10	90	88.0
CM-10–15	10	15	85	84.4
CM-10–20	10	20	80	84.7
CM-10–30	10	30	70	50.9
CM-5–15	5	15	85	76.2
CM-10–15	10	15	85	84.4
CM-20–15	20	15	85	92.7
CM-30–15	30	15	85	96.6

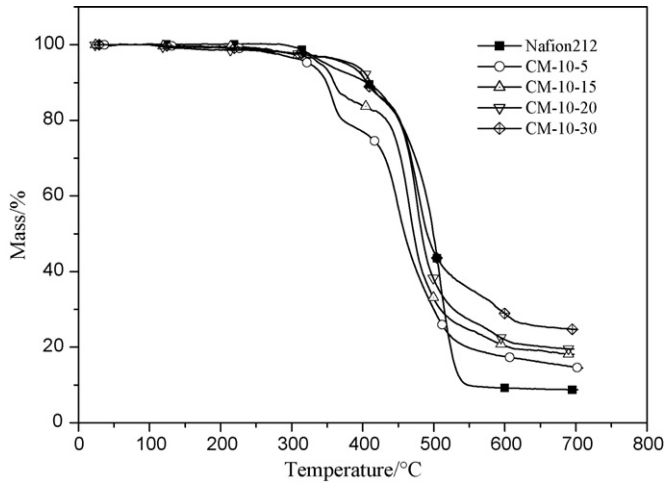

Fig. 6. Effects of the content of FPI-10 on degradation properties of CM-10–*Y*, nitrogen atmosphere.

3.3. Thermal properties of the composite membranes

The thermal stabilities of the composite membranes and Nafion®212 were studied by thermogravimetric analyzer (TGA) measurement from 20 °C to 700 °C at a heating rate of 10 °C min^{-1} under nitrogen atmosphere. Figs. 6 and 7 illustrate the typical TGA curves of the recast Nafion®212, CM-10–*Y*, and CM-*X*–15 membranes.

The recast Nafion®212 membrane showed two-step degradation in its TGA curve. The first one is around 329 °C, which is attributed to the decomposition of the sulfonic group. The second stage of degradation around 509 °C is due to the degradation of C–F in Nafion®212. For the composite membranes, they all exhibited a two-step degradation pattern, which was similar to that of Nafion®212. The first temperature of the weight loss of the composite membranes is in the range of 357–411 °C, which is higher than that of Nafion®212. The second step of the composite membranes over 450 °C indicates the degradation of the main chain of FPI and Nafion®212. This is a little lower than that of Nafion®212. Because the crosslinked FPI contains the aliphatic C–H bond whose thermal stability is not as good as that of the aliphatic C–F in Nafion®212. The residual mass at 700 °C of the composite membranes is higher than that of the recast Nafion®212 membrane. All these data indicates that the composite membranes show improved thermal stability compared to that of Nafion®212.

3.4. Mechanical properties of the composite membranes

The tensile strength of the composite membranes and pure Nafion®212 were examined at room temperature in dry state and the data are shown in Fig. 8. The tensile strength of the composite membrane is much higher than that of pure Nafion®212. Moreover, the tensile properties of CM-10–15 with crosslinked FPI is much higher than that of UCM-10–15 with uncrosslinked FPI. Because FPI was crosslinked during the membrane preparation and formed semi-IPN structure within the composite membranes, which could improve the tensile properties greatly. This also could prove that FPI is crosslinked in the membrane. The tensile strength of the composite membrane increases with increasing FPI contents, reaches the optimal value at 15% content, and decreases greatly when the

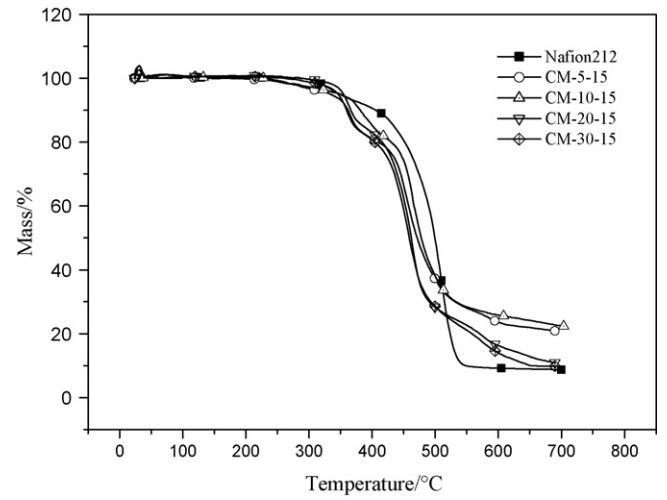

Fig. 7. Effects of the crosslinker content in FPI on degradation properties of CM-*X*–15, FPI content is 15%, nitrogen atmosphere.

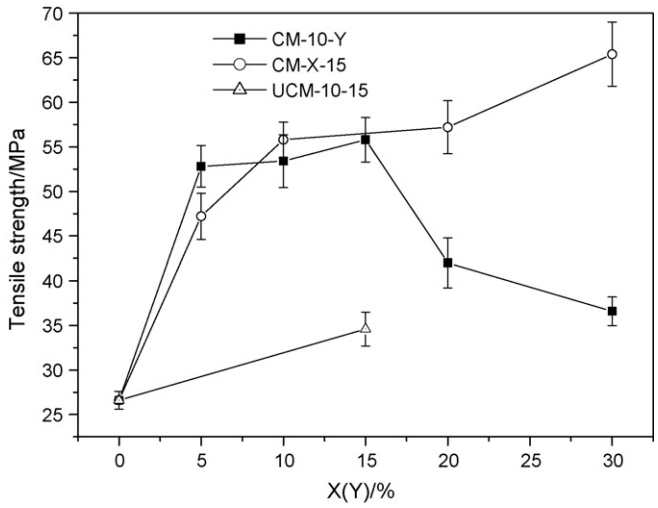

Fig. 8. Effects of the FPI-*X* contents in the composite membranes on the tensile strength of CM-10–*Y* and CM-*X*–15.

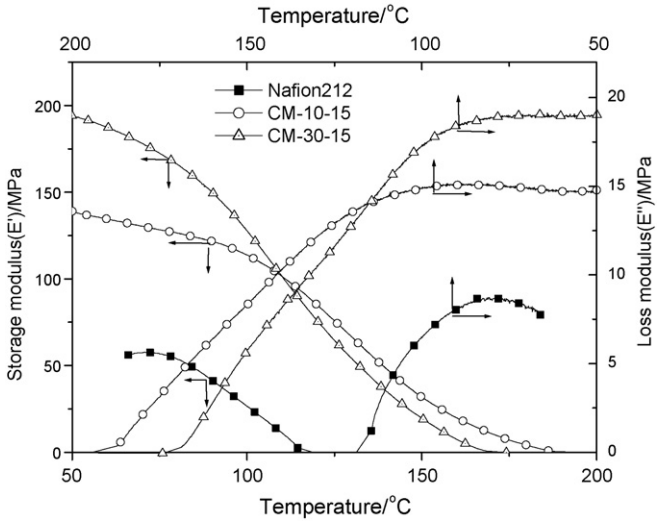

Fig. 9. Dynamic mechanical analysis (DMA) curves of CM-*X*–*Y* and Nafion®212.

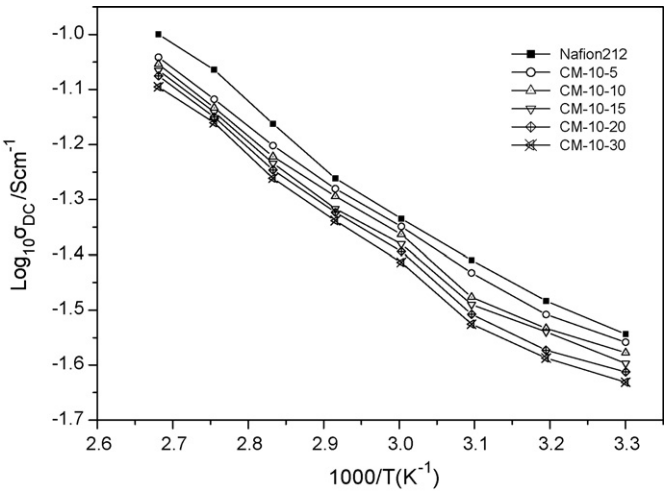

Fig. 10. Effects of the content of FPI-*X* on the proton conductivity of Nafion®212 and the composite membranes, relative humidity 100%.

content of FPI is higher than 15%. The composite membrane with FPI content higher than 30% is so brittle that it could not be tested. This might be due to the compatibility between Nafion®212 and FPI is getting worse when FPI content is higher. In addition, the tensile strength of CM-*X*–15 increases with increasing *X*. This is also due to the higher contents of reactive groups in CM-*X*–15 with higher *X* values.

Fig. 9 shows DMA results of Nafion®212, CM-10–15, and CM-30–15. The composite membranes have higher initial storage modulus than that of Nafion®212. From 50 °C to 118 °C, the change of the storage modulus for CM-10–15 (36%) and CM-30–15 (59%) is much smaller than that for Nafion®212 (100%). Both of the higher modulus and mechanical strength suggest better mechanical properties of the composite membranes than those of Nafion®212.

3.5. Water uptake and swelling ratio of the composite membranes

By dry–wet method, the water uptake and swelling ratio of the recast Nafion®212 and composite membranes were evaluated by immersed in deionized water and equilibrated for 48 h. Since PEMs in fuel cells are generally operated at temperature close to 80 °C, the water uptake and swelling ratio of pure and composite membranes were measured at 25 °C and 80 °C, respectively. The results are shown in Table 3. In general, the water uptake of the membranes increases with increasing temperature and increasing contents of the hydrophilic sulfonic groups. Compared with the recast Nafion®212, the composite membranes have lower water uptake at both 25 °C and 80 °C. This is due to the higher content of the sulfonic groups in pure Nafion®212 than that of the composite membranes. For the same reason, the water uptake of the composite membranes decreases with increasing content of FPI in CM-10–*Y*.

Table 3
Water uptake and swelling ratio of the composite membranes.

Membranes	Water uptake (%, w/w)		Swelling ratio (%)	
	25 °C	80 °C	25 °C	80 °C
Nafion®212	19.6	28.8	9.9	14.6
CM-10–5	11. 6	15.6	5.5	8.4
CM-10–10	10.8	14.9	4.9	7.3
CM-10–15	9.4	13.3	4.7	6.9
CM-10–20	8. 9	12.7	4.1	5.5
CM-10–30	7.9	11.7	2.3	3.7
CM-5–15	10.5	14.8	5.5	8.7
CM-10–15	9.4	13.3	4.7	6.9
CM-20–15	13.2	18.4	4.8	8.2
CM-30–15	10.5	19.3	4.7	8.9

The dimensional stability of the membranes was judged by the swelling ratio in this work. The lower the swelling ratio is, the better the dimensional stability is. The swelling ratio increases with increasing temperature, which is similar to that of the water uptake. The swelling ratio of the composite membranes is much lower than that of pure Nafion®212 and decreases with increasing content of FPI-*X*. This might be due to the decreased contents of the hydrophilic sulfonic groups and the introduction of the crosslinked FPI-*X*, which restrain the swelling of Nafion®212.

3.6. Proton conductivity of the composite membranes

Proton conductivity of the composite membranes was measured in 100% relative humidity by AC impedance spectroscopy. All the membrane samples were soaked in water over 24 h for hydration before measurement. Figs. 10 and 11 show the proton conductivity of the composite membranes with various FPI contents. The proton conductivity of the recast Nafion®212 membrane was also listed as a comparison. The proton conductivity of the composite membranes increases with increasing temperature, which is due to the

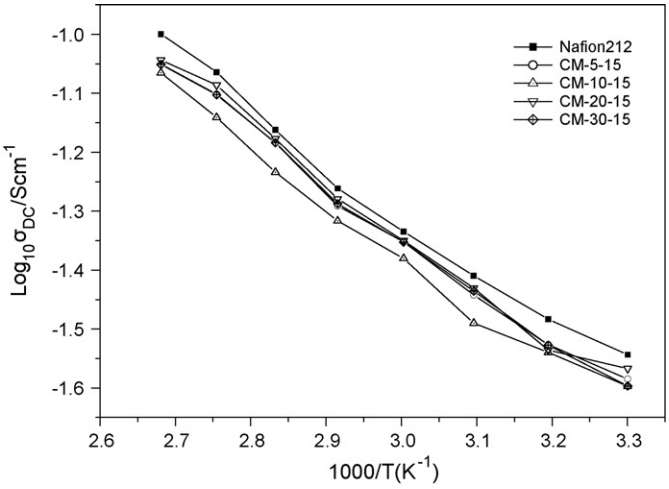

Fig. 11. Effects of the content of carboxyl groups in FPI on the proton conductivity of Nafion®212 and the composite membranes, relative humidity 100%.

more mobility of the proton and water molecules at higher temperature. The proton conductivity of the composite membranes is lower than that of pure Nafion®212, and decreases with increasing contents of FPI in CM-10–*Y*. The reason is that the content of sulfonic groups in the membranes was reduced and the dielectric properties as well as the hydrophobicity of polyimide have no contribution to the proton transport. For CM-*X*–15 series membranes, CM-20–15 has highest proton conductivity of 9.1×10^{-2} S cm^{-1} because of the highest water uptake. Therefore, all the composite membranes showed proton conductivity values over 10^{-2} S cm^{-1}, which indicate that they are suitable candidates for PEMs for fuel cell applications.

3.7. Oxidative stability of the composite membranes

The oxidative stability of the composite membranes was studied in Fenton reagent (30 ppm $FeSO_4$ in 30% H_2O_2) at 25 °C. It was characterized by the elapsed time (τ_1) when the membranes started to break into pieces after being drastically shaken. No composite membranes were broken when drastically shaken after being soaked in Fenton reagent for more than 3 months. This indicates that the composite membranes have good radical oxidative stability.

4. Conclusions

The reinforced composite membranes based on crosslinked fluorine-containing polyimide and Nafion®212 were successfully prepared through solution casting. The fluorine-containing polyimide was crosslinked during the membrane preparation and formed semi-IPN structure within the composite membrane. The mechanical properties of the composite membranes with semi-IPN structure were higher than that of the membranes from physical mixtures. The tensile strength of the composite membranes ranges from 36.6 to 65.4 MPa. CM-30–15 has the highest tensile strength of 65.4 MPa, which is more than twice of that of the recast Nafion®212 membrane (26.6 MPa). The initial storage modulus of CM-10–15 (139.1 MPa) is much higher than that of Nafion®212 membrane (56.1 MPa). The composite membranes exhibit excellent thermal and oxidative stability. The dimensional stability of the composite membrane is greatly improved than that of pure Nafion®212. The water uptake of the composite membranes is in the range of 11.7–19.3% at 80 °C and increases with increasing carboxyl content in the FPI-*X*. The proton conductivity of the composite membranes decreases with increasing FPI content, and is higher than 10^{-2} S cm^{-1}.

Acknowledgments

The project is sponsored by Natural Science Foundation of China (50773055); Post Doctoral Foundation of China (20080440640); Foundation for Nano Science & Technology of Shanghai (0852nm02200), Program for New Century Excellent Talents in University (NCET-06-0379).

References

[1] A. Regina, E. Fontananova, E. Drioli, M. Casciola, M. Sganappa, F. Trotta, J. Power Sources 160 (2006) 139–147.
[2] H.T. Pu, L. Qiao, Macromol. Chem. Phys. 206 (2005) 263–267.
[3] Y. Chen, H. Kim, J. Power Sources 190 (2009) 311–317.
[4] H.T. Pu, J. Wu, D.C. Wan, Z.H. Chang, J. Membr. Sci. 322 (2008) 393–399.
[5] C.Y. Chen, J.I.G. Rodriguez, M.C. Duke, R.F.D. Costa, A.L. Dicks, J.C.D. Costa, J. Power Sources 166 (2007) 324–330.
[6] H.L. Lin, T.L. Yu, L.N. Huang, L.C. Chen, K.S. Shen, G.B. Jung, J. Power Sources 150 (2005) 11–19.
[7] H.Y. Pan, X.L. Zhu, X.G. Jian, J. Membr. Sci. 326 (2008) 453–459.
[8] D. Sangeetha, Eur. Polym. J. 41 (2005) 2644–2652.
[9] X.M. Ren, T.E. Spinger, T.A. Zawodzinski, S.J. Gottesfeld, Electrochem. Soc. 147 (2000) 466–474.
[10] H.L. Lin, T.L. Yu, K.S. Shen, L.N. Huang, J. Membr. Sci. 237 (2004) 1–7.
[11] K. Ramya, G. Velayutham, C.K. Subramaniam, N. Rajalakshmi, K.S. Dhathathreyan, J. Power Sources 160 (2006) 10–17.
[12] F.Q. Liu, B.L. Yi, D.M. Xing, J.R. Yu, H.M. Zhang, J. Membr. Sci. 212 (2003) 213–223.
[13] Y.H. Liu, B.L. Yi, Z.G. Shao, D.M. Xing, H.M. Zhang, Electrochem. Solid-State Lett. 9 (2006) A356–A359.
[14] B.J. Landi, R.P. Raffaelle, M.J. Heben, J.L. Alleman, W. VanDerveer, T. Gennett, Nano Lett. 2 (2002) 1329–1332.
[15] R. Blake, Y.K. Gun'ko, J. Coleman, M. Cadek, A. Fonseca, J.B. Nagy, W.J. Blau, J. Am. Chem. Soc. 126 (2004) 10226–10227.
[16] R.M. Penner, C.R. Martin, J. Electrochem. Soc. 132 (1985) 514–515.
[17] M.W. Verbrugge, R.F. Hill, E.W. Schneider, AIChE J. 38 (1992) 93–100.
[18] C. Liu, C.R. Martin, J. Electrochem. Soc. 137 (1990) 510–515.
[19] C. Liu, C.R. Martin, J. Electrochem. Soc. 137 (1990) 3114–3120.
[20] H.T. Pu, L. Qiao, Q.Z. Liu, Z.L. Yang, Eur. Polym. J. 41 (2005) 2505–2510.
[21] X.L. Zhu, H.Y. Pan, Y.F. Liang, X.G. Jian, Eur. Polym. J. 44 (2008) 3782–3789.
[22] M. Paul, H.B. Park, B.D. Freeman, A. Roy, J.E. McGrath, J.S. Riffle, Polymer 49 (2008) 2243–2252.
[23] M.H. Jeong, K.S. Lee, J.S. Lee, Macromolecules 42 (2009) 1652–1658.
[24] Y. Gao, P.R. Gilles, D.G. Michael, G.Q. Wang, X.G. Jian, D.M. Serguei, X. Li, K. Serge, J. Membr. Sci. 278 (2006) 26–34.
[25] H.Y. Pan, Y.F. Liang, J.F. Li, X.L. Zhu, X.G. Jian, G.H. Xuan, Acta Polym. Sinica 8 (2007) 749–752.
[26] S. Xue, G.P. Yin, Polymer 47 (2006) 5044–5049.
[27] H.T. Pu, L.M. Tang, Polym. Int. 56 (2007) 121–125.